

# Task-driven SLAM Benchmarking for Robot Navigation

Yanwei Du<sup>1</sup>, Shiyu Feng<sup>2</sup>, Carlton G. Cort<sup>1</sup>, Patricio A. Vela<sup>1</sup>

**Abstract**—A critical use case of SLAM for mobile assistive robots is to support localization during a navigation-based task. Current SLAM benchmarks overlook the significance of repeatability (precision), despite its importance in real-world deployments. To address this gap, we propose a task-driven approach to SLAM benchmarking, *TaskSLAM-Bench*. It employs precision as a key metric, accounts for SLAM’s mapping capabilities, and has easy-to-meet implementation requirements. Simulated and real-world testing scenarios of SLAM methods provide insights into the navigation performance properties of modern visual and LiDAR SLAM solutions. The outcomes show that passive stereo SLAM operates at a level of precision comparable to LiDAR SLAM in typical indoor environments. *TaskSLAM-Bench* complements existing benchmarks and offers richer assessment of SLAM performance in navigation-focused scenarios. Publicly available code permits *in-situ* SLAM testing in custom environments with properly equipped robots.

**Keywords:** navigation, benchmark, precision, SLAM.

## I. INTRODUCTION

Service robots have increasingly been deployed into home and work environments, as well as other parts of daily life [1]–[7]. Their primary goal is to provide repeatable services that enhance productivity and foster more efficient work environments. Central to the operation of these mobile robots is SLAM, whose localization capabilities support navigation. A robust and reliable SLAM system is pivotal for completing tasks that are distributed throughout a given environment. Despite recent advancements in SLAM achieving high accuracy in existing benchmarks and datasets [8]–[11], service robots using SLAM for feedback continue to face challenges with robustness such that localization failures require human intervention to restore functionality [12]. These closed-loop failures are not adequately addressed by existing open-loop SLAM benchmarks, which means that performance in the former does not always translate to task-oriented autonomy performance. For service robots, the main concern is reliable navigation to the same location when needed, rather than highly accurate absolute positioning. Additional perception-based modules ensure completion of the service activity near the goal location. Consider that navigation benchmarks focus on robot terminal point performance, where success is defined by the robot reaching the goal region [13], [14]. A robot needs sufficient localization performance to reach the goal region. Of essence is reliable, repeatable performance

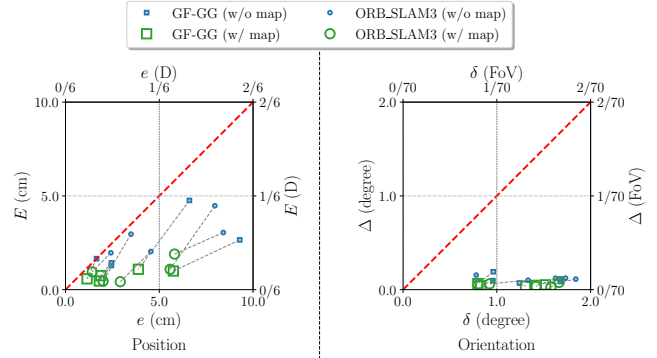


Fig. 1: Precision vs. Accuracy SLAM performance results without (w/o) and with (w) a map for EuRoC Machine Hall sequences. Each marker is a single sequence under a specific test mode. The dashed red line marks where precision equals accuracy. All data points being below this line suggest that accuracy under-reports task-repeatability. Metrics and units are defined in §II-B.2, with experimental details given in §III-C.

to ensure successful task execution every time. Repeatability, as measured using precision, is a common metric in robot automation [15]–[18]. This paper advocates to augment open-loop SLAM benchmarks with navigation-based SLAM benchmarks to better evaluate operational performance, and describes an easy to implement benchmarking scheme.

Real-world benchmarking with trajectory estimation error metrics remains mostly open-loop due to the metrics requiring absolute, global ground truth signals. Significant effort is required to obtain these signals. For instance, KITTI [8] uses RTK-GPS for precise vehicle positioning, and HILTI [9] employs a total station (e.g., a highly accurate laser scanner), both of which are costly. Datasets like EuRoC [10] and TUM [19] use motion-capture systems, which are difficult to implement in large-scale indoor, multi-room environments. For larger scale, multi-room environments, methods like PennCOSYVIO [20] use fiducial markers in conjunction with a laborious process involving meticulous placement and measurement of the markers. Sparser ceiling-mounted marker placement with total station surveying and an extra upwards facing camera on the robot can be a more effective approach for indoor settings. Other methods [21], [22] rely on LiDAR-SLAM or multi-sensor fusion results from an *offline pose optimization process* as ground truth. The proposed method removes the need for costly absolute measurement technology, labor-involved annotation, and offline pose optimization for ground truth.

The Subterranean (SubT) Challenge [23] was a real-world challenge requiring closed-loop implementation (e.g., SLAM and navigation integration) during exploration in underground environments with the objective of localizing targets distributed throughout them. It prioritized target de-

\*Supported in part by NSF Awards #1816138, 2235944, & 2345057.

<sup>1</sup>Y. Du, C. G. Cort, and P. A. Vela are with the School of Electrical and Computer Engineering, and Institute of Robotics and Intelligent Machines, Georgia Institute of Technology, Atlanta, GA 30308, USA. {yanwei.du, ccort6, pvela}@gatech.edu

<sup>2</sup>S. Feng is with the School of Mechanical Engineering and the School of Electrical and Computer Engineering, Georgia Institute of Technology, Atlanta, GA 30308, USA. shiyufeng@gatech.edu

tection and target position in an absolute global frame. The evaluation criteria emphasized giving the true location of the target rather than being able to reliably guide a human or robot back to the target. Resource intensive surveying methods were used to generate the ground truth.

While significant efforts have recently been devoted to rich, multi-sensor fusion capable benchmarking [9], [21], the performance gap between SLAM benchmarking via open-loop, sensor stream replay versus task-oriented performance has motivated other to evaluate SLAM and related autonomy modules through different lenses. Simulated worlds figure prominently due to reproducibility of outcomes, ease of implementation by researchers, and the availability of ground truth information. Embodied AI research, such as the Habitat Navigation Challenge [24], exemplifies the necessity for a task-driven evaluation methodology. The simulation-based challenge emphasizes the need for reliable, long-term navigation capabilities. The potential of localization to support autonomous vehicles has also led to the design of a simulation-based benchmarking scheme for street navigation [25] with success/failure as the main metric. SLAM latency plays a role in its robustness and accuracy, with some relationship found between these two factors for the task of trajectory tracking using SLAM pose estimates as feedback [26], [27]. The simulation-based benchmarking in [26], [27] demonstrate the need to move beyond just accuracy when considering SLAM in the closed-loop. A reasonable next step would be to more explicitly consider navigation.

An additional difference between these benchmarks and the deployment of service robots is that the latter often incorporate an initial mapping stage prior to being tasked. Existing benchmarks overlook this phase by evaluating performance solely through one-time data playback. SLAM maps are pivotal as they mitigate long-term drift and ensure consistency (high precision) across multiple visits to the same locations [28], [29]. Multi-session SLAM evaluation [30] does consider map reuse with accuracy metric for repeated runs to the same locations. However, the study design and variables may consider different performance factors and experimental methodology for LiDAR SLAM [30], and also for visual SLAM multi-map and map reuse open-loop tests [28], [29]. These works point to the need for reproducible and standardized benchmarking schemes for SLAM systems equipped with pre-built maps. Further evidence for this need is given in Fig. 1, where the EuRoC dataset is used in a multi-run manner (see §III-C for more details). The Precision vs Accuracy plots show better precision than accuracy indicating that SLAM evaluation may under-report performance. Including a mapping phase further improves performance, especially position precision. Referencing the performance metrics to robot characteristics (under  $x$ -axis) permits qualitative assessment of potential goal attainment success by relating precision to what task region the robot may see at its arrival pose.

This paper introduces a SLAM benchmark framework with navigation-in-loop that emphasizes task-relevant metrics such as repeatability (precision) and completion. The

benchmarking approach mimics real-world implementations where robots are typically given ample time to create a complete map for improved task execution during deployment. Through experiments on several visual and LiDAR SLAM methods, we identify which methods effectively support navigation tasks. The key contributions are as follows:

- A low-cost, easy to setup, task-driven SLAM benchmark with precision as the key metric for measuring robot consistency in reaching the same pose over multiple rounds. The method readily scales to large environments.
- Evaluation of stereo visual and LiDAR SLAM systems in simulation and real-world scenarios, with evidence that passive visual methods can match the robustness and precision of LiDAR-based methods for indoor settings.
- Open-sourced benchmarking code [31] for the robot autonomy community to easily test and evaluate task-driven SLAM in their own environments & on their own robots.

## II. METHODOLOGY

### A. Preliminaries

The following symbols and definitions are used:

- **Robot Pose** -  $(x, y, \theta)$  - Robot position and orientation.  $SE(3)$  pose estimates are projected to  $SE(2)$ .
- **Sequence** -  $\mathbf{S}$  - A set of waypoints the robot is required to sequentially follow, i.e.,  $\mathbf{S} = \{\mathbf{w}_1, \mathbf{w}_2, \dots, \mathbf{w}_N\}$ .
- **Waypoint** -  $\mathbf{w}_i = (x_i, y_i, \theta_i)$  indexed by  $i$  - position and orientation (heading angle) of the robot in the 2D plane.
- **Indexing** -  $i$  represents the waypoint index, and  $j$  the round index, and  $k$  the sequence index.
- **Counts** -  $N$  is the no. of waypoints in a sequence,  $M$  is the no. of rounds in a test, and  $K$  is sequence count.

Variables with a \* symbol indicate ground truth or reference values, while a  $\bar{\phantom{x}}$  symbol denotes mean value.

### B. Task-Driven SLAM Benchmarking Design

Mobile robot task execution requires SLAM to support collision-free navigation to designated target locations. Hence, the proposed SLAM benchmarking framework evaluates the use of closed-loop SLAM operation as part of navigation. Fig. 2 depicts the navigation system as implemented in ROS [32]. The navigation module uses TEB [33].

1) *Task Definition:* Waypoint Navigation. Waypoints represent task-relevant goal points, as exemplified in the AWS Gazebo hospital model [34] of Fig. 3. They are manually specified based on a floor plan of the environment's free space. It is assumed that the floor plan reflects the static environment, with no dynamic obstacles or unknown areas. The robot starts from a fixed location and sequentially navigates to each waypoint. Upon reaching a waypoint, the robot's pose is recorded for evaluation. The procedure is repeated for multiple rounds, terminating if the robot fails to reach any waypoint.

2) *Performance Metrics:* Accuracy, Completeness, and Precision. Typically, accuracy metrics such as Absolute Trajectory Error (ATE) or Relative Pose Error (RPE) are used to evaluate SLAM performance [19]. Navigation and trajectory

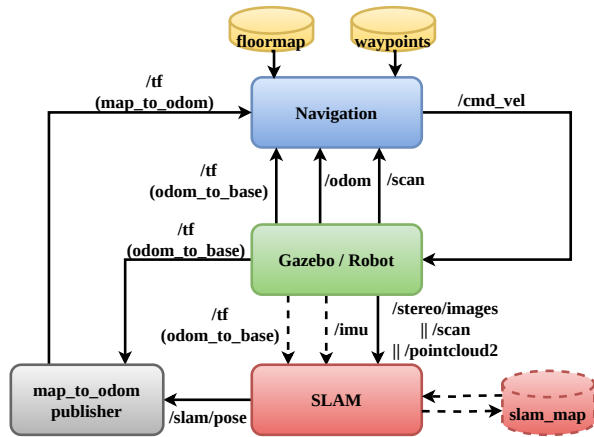


Fig. 2: Task-driven SLAM benchmarking design. Dashed arrows and cylinders represent optional elements specific to SLAM methods and test configurations. The || symbol denotes alternative robot sensor configurations.

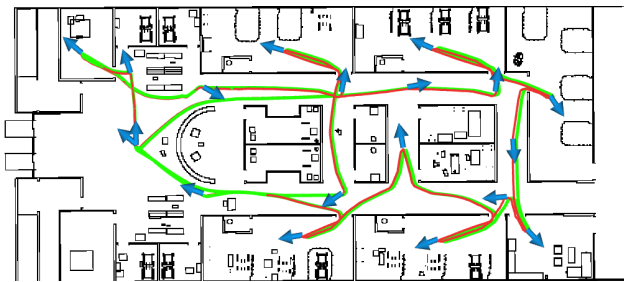


Fig. 3: Defined waypoints (blue arrows) in the AWS Gazebo hospital world, with the robot estimated trajectory (red) and ground truth trajectory (green) plotted when executing the navigation task.

tracking evaluation of SLAM employ task-specific metrics [25], [26]. Here, performance evaluation of indoor mobile robot navigation emphasizes waypoint navigation *reliability and repeatability*, measured by successful goal attainment percentage (completeness) and goal pose precision. Accuracy, in the form of APE, will apply for the simulated scenarios since ground-truth is available.

Navigation *accuracy* to waypoint  $\mathbf{w}_i$  captures how close the robot gets to the target goal over repeated rounds. It is based on the average position and orientation errors:

$$e_{\mathbf{w}_i} = \frac{1}{M} \sum_j \|\mathbf{z}_{ij} - \mathbf{z}_i^*\|_2 \quad \text{and} \quad \delta_{\mathbf{w}_i} = \frac{1}{M} \sum_j \|\theta_{ij} - \theta_i^*\|, \quad (1)$$

where  $\mathbf{z} = (x, y)$  and orientation error factors for wrap-around. Navigation *precision* at waypoint  $\mathbf{w}_i$  quantifies the proximity of robot pose measurements to each other over repeated rounds. Decomposed into position and orientation:

$$E_{\mathbf{w}_i} = \frac{1}{M} \sum_j \|\mathbf{z}_{ij} - \bar{\mathbf{z}}_i\|_2 \quad \text{and} \quad \Delta_{\mathbf{w}_i} = \frac{1}{M} \sum_j \|\theta_{ij} - \bar{\theta}_i\|, \quad (2)$$

where means are computed over all rounds (index  $j$ ).

Completeness ( $C$ ) refers to the ratio of completed waypoints over all waypoints across all sequences:

$$C = \frac{\sum_{k=1}^K \sum_{i=1}^{N_k} \delta_{ki}}{\sum_{k=1}^K N_k} \quad \text{for} \quad \delta_{ki} = \begin{cases} 0, & \text{if } M_{ki} < M \\ 1, & \text{otherwise} \end{cases} \quad (3)$$

where  $N_k$  is the waypoint count in sequence  $S_k$ , and  $M_{ki}$  is the successful waypoint  $\mathbf{w}_i$  attainment count for the  $M$  runs.

**Task-driven Units - ( $D, FoV$ ).** To emphasize performance from a task-driven perspective, outcomes will also report in unit scales relevant to the robot's physical characteristics:  $D$  the robot's diameter, and  $FoV$  the camera's horizontal field of view. These units to quantify position and orientation performance are robot-specific.

3) *Measuring Completeness and Precision:* Since the task-driven benchmark prioritizes waypoint precision, which assesses the repeatability of the robot's navigation across multiple rounds relative to its own internal (SLAM) coordinate system, there is no need to establish a global absolute coordinate system. Precision at each waypoint will be recovered from individual reference frames.

Waypoint precision measurement in real-world conditions may be obtained in two equivalent manners similar to virtual reality systems: outside-in or inside-out. Outside-in uses a downward facing camera from a suitable height (Fig. 4). Options include overhead/ceiling-mounted, tripod-installed, or otherwise placed to face the ground region the robot is expected to reach. Each camera requires connection to a (low cost) computer or laptop to estimate the robot's pose upon reaching the waypoint. An AprilTag is affixed to the top of the robot for pose estimation from the camera system (Fig. 4). AprilTag detection validation [35] indicates point error is within 0.5 pixel for the AprilTag C++ library, making it suitable for evaluation purposes. Inside-out operates as in [36] by inverting the setup. An upwards-facing camera is placed on the robot and tags are placed in the environment.

Importantly, waypoint precision does not rely on absolute references. It is assessed independently of other waypoints, and the evaluation is possible in local coordinate systems defined by the cameras observing them. The outside-in approach does not require global calibration of the camera poses (nor relative poses). Each camera/waypoint measurement pair operates independently. The inside-out approach does not require a global scan nor globally aligned tags. Lastly, waypoint attainment success is established by the tag being fully visible to the camera, otherwise the robot failed to reach the waypoint's vicinity.

From a task-driven perspective, as long as the robot can successfully transit to subsequent tasks, achieving high accuracy is less critical. Instead, high precision indicates that the robot consistently navigates to the target location in its internal SLAM coordinate system, which is better aligned with the needs of practical applications. This method offers a significant testing advantage. Both setups are straightforward and easy to install at the necessary measurement areas. They do not require global calibration, specialized expertise, nor expensive specialized equipment for operation (as required for a motion capture system or a surveying strategy). Since simulation experiments provide accuracy and precision from simulator ground truth information, they provide understanding of how these two metrics relate in a given environment.

4) *Map-Based Performance Evaluation:* To demonstrate the impact of map reuse on task completion, we run addi-

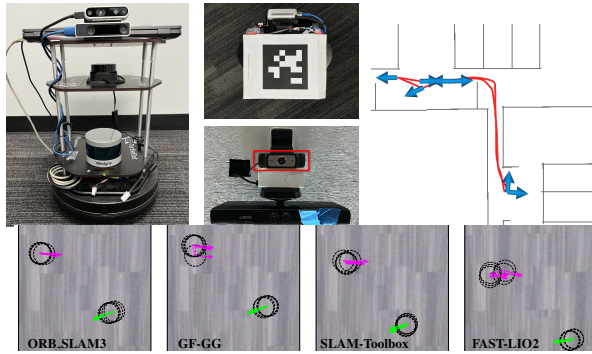


Fig. 4: Real-world experimental setup. Clock-wise from top-left: A Turtlebot2 is equipped with the SLAM sensors and laptop, on top of which is placed an AprilTag. Downward facing cameras (in red box) and computers/laptops are placed in the environment to detect and recover the robot’s pose. The robot waypoints, defined to be under the cameras, should be accurate enough that the robot will be visible when reached. During the programmed tour, the cameras will detect and estimate the robot pose when seen. Precision and Completeness follows from the estimates. The lower figure presents an example of the robot captured at two waypoints (magenta and green) for different SLAM methods. Arrows indicate orientation and black circles indicates position, over multiple runs.

tional tests for SLAM methods that support mapping. Since some methods cannot save and load maps, we introduce an extra priming round where the robot traverses the waypoints and builds a map online. This map is then used for subsequent rounds without resetting the robot’s pose to the initial location after each round. The robot poses recorded during the mapping phase are excluded from evaluation. Comparing the results from tests with and without the use of a pre-built SLAM map highlights the benefits of a prior SLAM map for task-oriented SLAM performance.

### III. EXPERIMENT DESIGN

The effectiveness of the proposed benchmark framework will be established through a series of controlled experiments. Simulation experiments assess SLAM performance using all metrics: Accuracy, Precision, and Completeness. Plots will include dual axes with standard units and robot-relative units to link performance directly to the robot’s physical characteristics and task requirements. If a robot is too far from an object, relative to its size, or headed in a bad direction, relative to its visual field of view, then a follow-up visually guided manipulation, inspection/object viewing, or other task would fail.

#### A. SLAM Candidates

To demonstrate the flexibility of the benchmark and support comparative analysis, several SLAM methods are tested. They include inertial and robot odometry signals as required or when permitted. SLAM parameters were not tuned for optimal performance across the tests, with default settings used; they are generally effective in most scenarios and offer balanced performance. Our goal is not to identify the best SLAM method, but rather to demonstrate the functionality of the proposed SLAM benchmarking design (*TaskSLAM-Bench*), and to use the demonstration to assess which SLAM methods are suitable for task-driven purposes. Tested are:

TABLE I: Scenario Properties in Simulation and Real-World

Name	Key Features	Area ( $m^2$ )	Path Length ( $m$ )
Small House	Home furniture layouts	144	45
Warehouse	Shelves with boxes & goods	260	70
Hospital	Rooms w/medical equipment	1400	220
TSRB Office	Multiple long corridors	1500	260
TSRB Short	A long corridor and sharp turns	225	45
TSRB Long	Long distance loop closures	620	120

1) *2D LiDAR*: SLAM-Toolbox [37] and HectorSLAM [38]. They leverage scan matching to correct robot odometry drift and are commonly used for indoor navigation.

2) *Stereo Visual and Visual-Inertial*: GF-GG [27] & ORB\_SLAM3 [28], feature-based stereo visual methods; DSOL [39], a direct sparse odometry system; SVO-Pro [40], a semi-direct method; and MSCKF [41], a filter-based method. ORB\_SLAM3 would often fail to initialize when using inertial measurements, even with extra movement prior to testing. It is run as stereo-only.

3) *3D LiDAR-Inertial*: FAST-LIO2 [42] and LIO-SAM [43]. They are commonly deployed for autonomous driving, and were used by SubT Challenge competitors [44], [45].

#### B. SLAM-in-the-Loop Navigation Experiments

Testing involves both simulated and real-world environments, whose scenarios are described in Table I. In each scenario, the robot starts from a fixed initial location, typically the origin of the map, and navigates sequentially through the waypoints. The navigation system configuration is fixed across all experiments. Upon reaching each waypoint, the robot pauses for 5 seconds before proceeding to the next one. For an outside-in setup, the computer/laptop at this waypoint, synchronized with NTP (delay  $< 1$  second), saves timestamped image data upon detecting the tag affixed to the robot. The robot’s poses are estimated offline and associated with waypoints by timestamp for performance evaluation.

A single scenario is tested for five consecutive rounds. In each round, the robot is either reset or continues based on the testing modes—without and with a SLAM map. The same resetting strategy is applied to all SLAM methods tested. A waypoint is considered successfully completed only if the robot arrives at it in all five rounds; failure to reach a waypoint in any round leads to the incomplete classification. Accuracy, if available, and precision for each completed waypoint is calculated according to Eqns. (1) and (2).

The testing platform is a Turtlebot 2 robot, shown in Fig. 4, which offers odometry measurements through built-in sensors. Mounted to it are an RPLiDAR S2 for 2D LiDAR-based SLAM methods, a Realsense D435i (FoV:  $87^\circ$ ) for visual (and visual-inertial) methods, and a Velodyne-16 for 3D LiDAR SLAM methods. The laser data also feeds to the navigation module for obstacle avoidance. All the processes run on an Intel Core i7-9850 laptop (single-thread passmark score of 2483). The simulation robot is similarly configured. The task-driven units use  $D = 30$  cm and  $FoV = 80.0^\circ$ .

1) *Simulation*: Gazebo [46] is chosen for the simulation benchmark testing. It provides readily available sensor setups

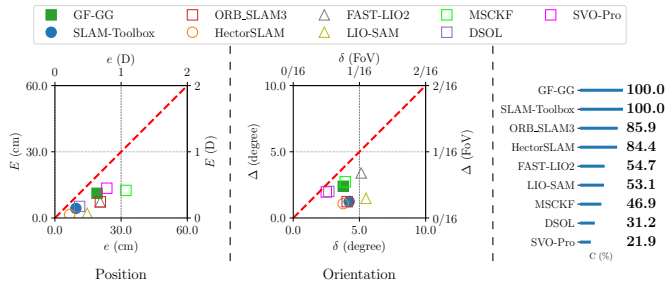


Fig. 5: Simulation SLAM Precision vs. Accuracy in tests w/o map. Methods with 100% waypoint completeness have filled markers. The dashed red line denotes precision equal to accuracy. Markers below this line mean that accuracy under-reports task-repeatability performance. Completeness values are represented as a bar plot on the right (longer is better).

(i.e., camera and LiDAR feeds) and ground-truth data for measuring accuracy and precision.

2) *Real World*: Real-world testing was performed in an office environment. One test defined a path sequence of  $\sim 45$  meters in length and featuring six waypoints, see Fig. 4. It has short stretches in a corridor, sharp turns, and return loops. Using an outside-in approach, three overhead cameras (Fig. 4) captured the robot for success determination and precision measurements. Another test, with the inside-out approach, defined a travel sequence of about 120 meters in length with twelve waypoints. It has similar properties to the first test but over longer distances.

### C. Open-Loop EuRoC Evaluation - A Preliminary Study

This section describes the performance evaluation performed for the provisional SLAM performance analysis noted in the Introduction, which argued that performance evaluation would benefit from including task-driven evaluation. The EuRoC machine hall sequences may be interpreted as an aerial vehicle inspection task; the objective is to consistently revisit specific points during repeat inspections. Evaluation involves pose estimation accuracy and precision, with each frame treated as an inspection point to reach.

1) *Setup*: Two stereo SLAM methods, ORB\_SLAM3 and GF-GG, are tested. For *w/map*, each sequence restarts without resetting the SLAM method to keep the map in memory for subsequent runs. Eqns. (1) and (2) are modified for evaluation in  $SE(3)$ . Based on [10], task-driven units are set to  $D = 30\text{cm}$  and  $FoV = 70.0^\circ$ .

2) *Results and Analysis*: Fig. 1 visualizes the results as Precision vs. Accuracy plots. Given that the red dashed line is precision-accuracy parity, position precision values match or are lower than accuracy values across all sequences. Orientation precision is noticeably better than accuracy. The results exhibit better localization repeatability than absolute accuracy would suggest. When utilizing a SLAM map, both methods exhibit an improved performance with outcomes shifted toward the lower-left corner. Position precision error, which is within  $1/6$  of a robot diameter in *w/o map* tests, reduces to  $1/12$  of a robot diameter in *w/map* tests. Orientation precision error, at  $1/35 FoV$ , reduces by a factor of 10 in the *w/map* tests (to pixel level error). An object intended to be centered in the field of view from a reasonable distance

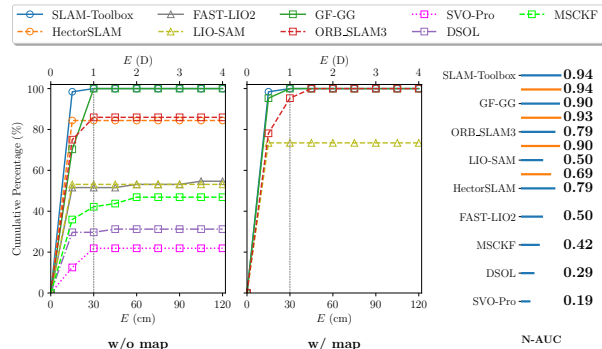


Fig. 6: Cumulative Position Precision plots for tests w/o-and w-map in simulation. Normalized area-under-curve for each method in both modes, shown as a bar plot on the right. Blue lines: w/o-map; orange lines: w-map. Longer bars indicate better performance.

would still be visible and nearly centered. This suggests that accuracy does not fully reflect potential SLAM performance from a task-driven perspective, and points towards the benefits of *augmenting* it with precision.

### D. Task-Driven SLAM Benchmark Outcomes and Analysis

Simulation outcomes will first be analyzed, including precision/accuracy comparison. Real-world outcomes will then be analyzed. Following [39], performance analysis will include cumulative precision plots (see Figs. 6 and 8). The curve traces the percentage of waypoints with a precision error value less than the equivalent  $x$ -axis threshold. The normalized area-under-curve (N-AUC) for the cumulative plots provides an overall performance score for each method. A higher N-AUC indicates better performance, with curves closer to the top-left corner representing superior precision and completeness. The analysis points to precision as a meaningful metric to pair with completeness, and to passive stereo SLAM as being on par with LiDAR-based SLAM.

1) *Simulation*: Fig. 5 Precision vs. Accuracy plots in without map tests for position and orientation consistently show lower precision value than accuracy when the navigation succeeds. To some degree this indicates that localization failure is catastrophic when it occurs; there doesn't seem to be a sliding scale. The cumulative position precision plot in Fig. 6 indicates the same by plateauing rather than exhibiting linear growth to 100% across the precision axis. In the cases studied, either a SLAM method is precise to a robot diameter or it fails. Orientation accuracy and precision values are low given the field of view. Due to the strong performance of orientation, it will not be reviewed in future analyses.

The least complete implementations are odometry methods (DSOL, SVO-Pro), MSCKF and as they cannot leverage map content, nor long baseline associations outside of the filtering window. The two 3D-LiDAR methods performed comparably in the *w/o map* tests. However, they did not match 2D-LiDAR performance. This performance contrasts with their near universal preference in robot deployments [23], which may be due to the heavy emphasis on *exploration* rather than repeatable navigation. Exploration has looser navigation demands. HectorSLAM and ORB\_SLAM3 were

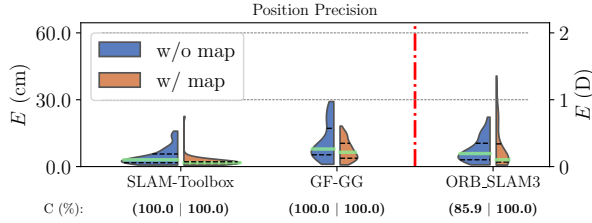


Fig. 7: Distribution of Waypoint Position Precision for tests without (w/o) and with (w/) map in simulation. The vertical red dash-dotted line marks the boundary for full completeness. Each distribution bar contains the mean (solid green line) and quartiles (black dashed lines).

closer to perfect, but exhibit enough failures to not be reliable. One visual SLAM method, GF-GG, matched the perfect completeness performance of the 2D-LiDAR SLAM-Toolbox implementation. Both achieved 100% cumulative precision at one robot diameter, indicating that the two methods are comparable in performance, though SLAM-Toolbox has an edge in the N-AUC score.

Using a map improves performance as seen in Fig. 6 by the upwards and/or leftwards shift of plotted curves relative to the w/o map curve. Correspondingly, the N-AUC scores improve. SLAM-Toolbox shows minimal change, primarily due to its scan-to-map registration design, which is well-suited for indoor scenarios, and its continuous pose-graph-based global map management. ORB\_SLAM3’s imperfect w/o map completion becomes perfect w/map completion. It has the lowest N-AUC score relative to SLAM-Toolbox and GF-GG, and hits perfect completion at around 1.5D.

The Fig. 7 violin plots depict the distribution of position precision for SLAM-Toolbox and the stereo SLAM methods. For SLAM-Toolbox and GF-GG, map use concentrates the distribution at lower values. While SLAM-Toolbox has four times lower mean precision error (1.75 cm vs. 6.41 cm), both have similar performance from a task perspective.

2) *Real-World*: Analysis will focus only on position precision, as the average orientation precision value lies below 10 degrees for all methods. Being at 1/8 of the camera’s field of view, this level of orientation precision is acceptable from a task-driven perspective. Fig. 8 provides cumulative position precision plots for the real-world tests (w/o and w/map). HectorSLAM, DSOL, and MSCKF did not perform well enough to warrant inclusion (below 20%). Performance of the other implementations roughly matches the ordering of simulation, with SLAM-Toolbox and GF-GG achieving perfect completion but at around 2 robot diameters, which may influence the robot’s ability to perceive the task workspace region upon arrival. The LIO methods and ORB\_SLAM3 achieved high completion rates. Passive stereo implementations continue to exhibit comparable performance to LiDAR-based implementations.

Moving to the Fig. 8 w/map case, there is a left-ward shift in the curve indicating improved precision and an overall compression in pose variance across methods. The violin plots of Fig. 8 (top), support this same finding. Only SLAM-Toolbox manages 100% completion, with the others failing on the second long distance test. The stereo SLAM methods

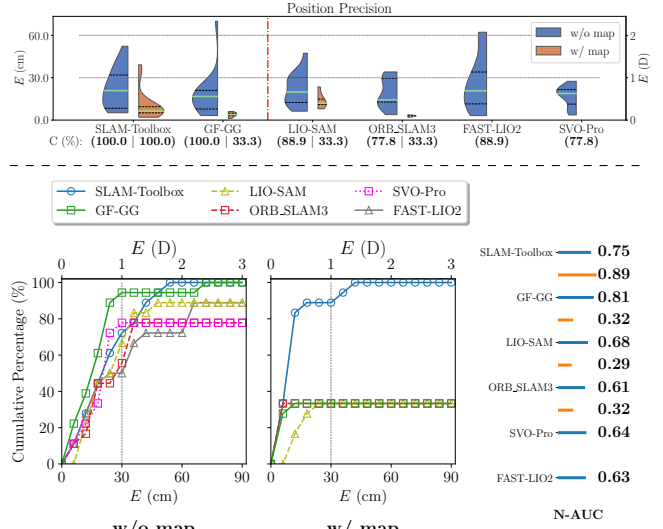


Fig. 8: Top: Distribution of Waypoint Position Precision for tests without (w/o) and with (w/) map in real-world. The legends and settings are consistent with Fig. 7. Bottom: Cumulative Position Precision Plot of real-world test data with the same legends and settings as Fig. 6.

failures are programmatic (program crashes), arising from issues managing the visual map over long time-and large spatial-scales, especially when there are periods of poor visual conditions. They achieved perfect performance on the short run test; for those runs GF-GG and ORB\_SLAM3 matched SLAM-Toolbox with an N-AUC of 0.93 and 0.95 vs 0.92. The violin plots of GF-GG and ORB\_SLAM3 consist of only the short run test. The degraded long-term performance indicates that future improvements should be aimed at back-end elements (long-term mapping, graph maintenance, and keyframe culling). Resolving these bugs may lead to performance matching that of SLAM-Toolbox. The multimedia attachment provides visual evidence from the cameras to qualitatively see how precision varies across the methods.

3) *Discussion*: The entirety of *TaskSLAM-Bench* results reveal that Visual SLAM achieves performance approaching that of LiDAR SLAM in closed-loop navigation tasks, a finding not captured by existing benchmarks. These results demonstrate that vision-based approaches are capable of delivering strong navigation performance once robust program execution is achieved. Using a SLAM map with map-to-frame tracking significantly improves performance. It reduces drift and enhances long-term consistency, which has positive impacts on maintaining robust and accurate navigation.

Long-path tests reveal that LiDAR SLAM scales more effectively to large environments and handles feature-less scenarios better than visual methods. It excels in structured settings, leveraging geometric features for robust loop closure and an efficient occupancy-grid map representation. Visual SLAM has issues with bounded map maintenance and feature poor areas (e.g., long corridors), highlighting the need for multisensor fusion to enhance robustness.

Overall, GF-GG outperforms ORB\_SLAM3 by prioritizing efficient map-to-frame tracking and local BA, suggesting

scalability improvements are critical to long-term SLAM. Better integrating robot odometry into the pose graph design can enhance robustness in degenerate, feature poor scenarios to ensure continuous operation.

#### IV. CONCLUSION

This work introduces a task-driven SLAM benchmark, whose focus on precision highlights its importance in task-oriented applications where repeatability is essential. It considers the SLAM system mapping capabilities, an aspect often overlooked in existing evaluations, but which provides a more comprehensive understanding of SLAM performance and suitability for real-world tasks. *TaskSLAM-Bench* results show that visual SLAM methods can achieve precision performance comparable to LiDAR-based methods in indoor navigation tasks. Further effort is needed to resolve large-scale visual maps. This finding underscores the potential of visual SLAM systems to be reliable and effective alternatives to LiDAR approaches. The benchmark itself is low-cost and easy to implement. Other researchers may test their robots in their own environments with a given SLAM implementation.

#### REFERENCES

- [1] Z. A. Barakeh, S. Alkork, A. S. Karar, S. Said, and T. Beyrouthy, "Pepper humanoid robot as a service robot: a customer approach," *3rd International Conference on Bio-engineering for Smart Technologies*, pp. 1–4, 2019.
- [2] Amazon Astro. [Online]. Available: <https://www.aboutamazon.com/news/tag/astro>
- [3] B. Tribelhorn and Z. Dodds, "Evaluating the Roomba: A low-cost, ubiquitous platform for robotics research and education," in *IEEE International Conference on Robotics and Automation*, 2007, pp. 1393–1399.
- [4] Moxi. Diligent Robotics. [Online]. Available: <https://www.diligentrobots.com/moxi>
- [5] M. Valdez, M. Cook, and S. Potter, "Humans and robots coping with crisis – starship, covid-19 and urban robotics in an unpredictable world," in *IEEE International Conference on Systems, Man, and Cybernetics (SMC)*, 2021, pp. 2596–2601.
- [6] M. Barten. Hotel Robots: An Overview of Different Robots Used in Hotels. [Online]. Available: <https://www.revfine.com/hotel-robots>
- [7] Knightscope Inc. [Online]. Available: <https://www.knightscope.com>
- [8] A. Geiger, P. Lenz, and R. Urtasun, "Are we ready for autonomous driving? the KITTI vision benchmark suite," in *IEEE Conference on Computer Vision and Pattern Recognition*, 2012, pp. 3354–3361.
- [9] M. Helmberger, K. Morin, B. Berner, N. Kumar, G. Cioffi, and D. Scaramuzza, "The hilti slam challenge dataset," *IEEE Robotics and Automation Letters*, vol. 7, no. 3, pp. 7518–7525, 2022.
- [10] M. Burri, J. Nikolic, P. Gohl, T. Schneider, J. Rehder, S. Omari, M. Achtelik, and R. Y. Siegwart, "The EuRoC micro aerial vehicle datasets," *The International Journal of Robotics Research*, vol. 35, pp. 1157 – 1163, 2016.
- [11] T. Schops, T. Sattler, and M. Pollefeys, "Bad slam: Bundle adjusted direct rgb-d slam," in *IEEE/CVF Conference on Computer Vision and Pattern Recognition*, 2019, pp. 134–144.
- [12] L. Young. (2024, January) Companies Brought in Robots. Now They Need Human 'Robot Wranglers'. [Online]. Available: <https://www.warehouseautomation.ca/news/companies-brought-in-robots-now-they-need-human-robot-wranglers>
- [13] J. S. Smith, S. Feng, F. Lyu, and P. A. Vela, "Real-Time Egocentric Navigation Using 3D Sensing," *Machine Vision and Navigation*, 2019.
- [14] S. Feng, F. Lyu, J. H. Hwang, and P. A. Vela, "Ego-centric stereo navigation using stixel world," in *IEEE International Conference on Robotics and Automation*, 2021, pp. 13 201–13 207.
- [15] X. Zhang, W. Tian, L. Wang, and T. Huang, "Evaluation and prediction method of robot pose repeatability based on statistical distance," *Mechanism and Machine Theory*, vol. 179, p. 105122, 2023.
- [16] M. Płaczek and Łukasz Piszczek, "Testing of an industrial robot's accuracy and repeatability in off and online environment," *Eksploatacja i Niezawodność - Maintenance and Reliability*, 2018.
- [17] What is Repeatability in Robotics. [Online]. Available: <https://www.awerobotics.com/home/what-is-repeatability-in-robotics/>
- [18] Robot precision vs accuracy: Understanding the differences. [Online]. Available: <https://standardbots.com/blog/robot-precision>
- [19] J. Sturm, N. Engelhard, F. Endres, W. Burgard, and D. Cremers, "A benchmark for the evaluation of RGB-D SLAM systems," in *IEEE/RSJ international conference on intelligent robots and systems*, 2012, pp. 573–580.
- [20] B. Pfrommer, N. Sanket, K. Daniilidis, and J. Cleveland, "Pen-COSYVIO: A challenging visual inertial odometry benchmark," in *IEEE International Conference on Robotics and Automation*, 2017, pp. 3847–3854.
- [21] P. Kaveti, A. Gupta, D. Giaya, M. Karp, C. Keil, J. Nir, Z. Zhang, and H. Singh, "Challenges of Indoor SLAM: A multi-modal multi-floor dataset for SLAM evaluation," in *IEEE International Conference on Automation Science and Engineering*, 2023, pp. 1–8.
- [22] P. Wenzel, R. Wang, N. Yang, Q. Cheng, Q. A. Khan, L. von Stumberg, N. Zeller, and D. Cremers, "4Seasons: A Cross-Season Dataset for Multi-Weather SLAM in Autonomous Driving," *Pattern Recognition*, vol. 12544, pp. 404–417, 2020.
- [23] T. H. Chung, V. Orekhov, and A. Maio, "Into the Robotic Depths: Analysis and Insights from the DARPA Subterranean Challenge," *Annual Review of Control, Robotics, and Autonomous Systems*, vol. 6, no. 1, pp. 477–502, 2023.
- [24] K. Yadav, J. Krantz, R. Ramrakhya, S. K. Ramakrishnan, J. Yang, A. Wang, J. Turner, A. Gokaslan, V.-P. Berges, R. Mootaghi, O. Maksymets, A. X. Chang, M. Savva, A. Clegg, D. S. Chaplot, and D. Batra. Habitat Challenge 2023. [Online]. Available: <https://aihabitat.org/challenge/2023/>
- [25] L. Suomela, J. Kalliola, A. Dag, H. Edelman, and J.-K. Kämäräinen, "Benchmarking Visual Localization for Autonomous Navigation," in *IEEE/CVF Winter Conference on Applications of Computer Vision*, 2023, pp. 2945–2955.
- [26] Y. Zhao, J. S. Smith, S. H. Karumanchi, and P. A. Vela, "Closed-loop benchmarking of stereo visual-inertial SLAM systems: Understanding the impact of drift and latency on tracking accuracy," in *IEEE International Conference on Robotics and Automation*, 2020, pp. 1105–1112.
- [27] Y. Zhao, J. S. Smith, and P. A. Vela, "Good Graph to Optimize: Cost-Effective, Budget-Aware Bundle Adjustment in Visual SLAM," *ArXiv*, vol. abs/2008.10123, 2020.
- [28] C. Campos, R. Elvira, J. J. G. Rodríguez, J. M. M. Montiel, and J. D. Tardós, "ORB-SLAM3: An Accurate Open-Source Library for Visual, Visual-Inertial, and Multimap SLAM," *IEEE Transactions on Robotics*, vol. 37, no. 6, pp. 1874–1890, 2021.
- [29] R. Mur-Artal and J. D. Tardós, "Visual-Inertial Monocular SLAM With Map Reuse," *IEEE Robotics and Automation Letters*, vol. 2, no. 2, pp. 796–803, 2017.
- [30] E. Pearson and B. Englot, "A Robust and Rapidly Deployable Waypoint Navigation Architecture for Long-Duration Operations in GPS-Denied Environments," in *20th International Conference on Ubiquitous Robots*, 2023, pp. 319–326.
- [31] Task Driven SLAM Benchmarking. [Online]. Available: [https://github.com/ivalab/task\\_driven\\_slam\\_benchmarking.git](https://github.com/ivalab/task_driven_slam_benchmarking.git)
- [32] M. Quigley, K. Conley, B. Gerkey, J. Faust, T. Foote, J. Leibs, R. Wheeler, and A. Y. Ng, "ROS: an open-source robot operating system," in *IEEE International Conference on Robotics and Automation workshop on open source software*, vol. 3, no. 3.2, 2009, p. 5.
- [33] C. Rösmann, W. Feiten, T. Wösch, F. Hoffmann, and T. Bertram, "Efficient trajectory optimization using a sparse model," in *European Conference on Mobile Robots*, 2013, pp. 138–143.
- [34] AWS Gazebo Model. [Online]. Available: <https://github.com/aws-robotics/aws-robomaker-hospital-world.git>
- [35] S. M. Abbas, S. Aslam, K. Berns, and A. Muhammad, "Analysis and improvements in apriltag based state estimation," *Sensors*, vol. 19, no. 24, p. 5480, 2019.
- [36] H. Kikkeri, G. Parent, M. Jalobeanu, and S. Birchfield, "An inexpensive method for evaluating the localization performance of a mobile robot navigation system," *IEEE International Conference on Robotics and Automation*, pp. 4100–4107, 2014.
- [37] S. Macenski and I. Jambrecic, "SLAM Toolbox: SLAM for the dynamic world," *Journal of Open Source Software*, vol. 6, no. 61, p. 2783, 2021.

- [38] S. Kohlbrecher, O. Von Stryk, J. Meyer, and U. Klingauf, "A flexible and scalable SLAM system with full 3D motion estimation," in *IEEE international symposium on safety, security, and rescue robotics*, 2011, pp. 155–160.
- [39] C. Qu, S. S. Shivakumar, I. D. Miller, and C. J. Taylor, "DSOL: A Fast Direct Sparse Odometry Scheme," in *IEEE/RSJ International Conference on Intelligent Robots and Systems*, 2022, pp. 10587–10594.
- [40] C. Forster, Z. Zhang, M. Gassner, M. Werlberger, and D. Scaramuzza, "SVO: Semidirect visual odometry for monocular and multicamera systems," *IEEE Transactions on Robotics*, vol. 33, no. 2, pp. 249–265, 2016.
- [41] A. I. Mourikis and S. I. Roumeliotis, "A multi-state constraint Kalman filter for vision-aided inertial navigation," in *IEEE International Conference on Robotics and Automation*, 2007, pp. 3565–3572.
- [42] W. Xu, Y. Cai, D. He, J. Lin, and F. Zhang, "FAST-LIO2: Fast Direct LiDAR-Inertial Odometry," *IEEE Transactions on Robotics*, vol. 38, pp. 2053–2073, 2021.
- [43] T. Shan, B. Englot, D. Meyers, W. Wang, C. Ratti, and D. Rus, "LIO-SAM: Tightly-coupled Lidar Inertial Odometry via Smoothing and Mapping," *IEEE/RSJ International Conference on Intelligent Robots and Systems*, pp. 5135–5142, 2020.
- [44] K. Ebadi, L. Bernreiter, H. Biggie, G. Catt, Y. Chang, A. Chatterjee, C. Denniston, S.-P. Deschênes, K. Harlow, S. Khattak, L. Nogueira, M. Palieri, P. Petr'avecsek, M. Petrl'ik, A. Reinke, V. Kr'atk'y, S. Zhao, A. akbar Agha-mohammadi, K. Alexis, C. Heckman, K. Khosoussi, N. Kottege, B. Morrell, M. Hutter, F. Pauling, F. Pomerleau, M. Saska, S. A. Scherer, R. Y. Siegwart, J. L. Williams, and L. Carlone, "Present and Future of SLAM in Extreme Underground Environments," *ArXiv*, vol. abs/2208.01787, 2022.
- [45] A. Koval, C. Kanellakis, and G. Nikolakopoulos, "Evaluation of Lidar-based 3D SLAM algorithms in SubT environment," *IFAC-PapersOnLine*, vol. 55, no. 38, pp. 126–131, 2022.
- [46] N. Koenig and A. Howard, "Design and use paradigms for Gazebo, an open-source multi-robot simulator," in *IEEE/RSJ International Conference on Intelligent Robots and Systems*, vol. 3, 2004, pp. 2149–2154.